




Spring 5-2-2017

Characterizing TMX and chemotactic receptor arrays through bacterial two-hybrid and beta-galactosidase assays

Adam Keith Hubler
ahubler@vols.utk.edu

Follow this and additional works at: https://trace.tennessee.edu/utk_biocpubs

 Part of the [Molecular Biology Commons](#)

Recommended Citation

Hubler, Adam Keith, "Characterizing TMX and chemotactic receptor arrays through bacterial two-hybrid and beta-galactosidase assays" (2017). *Faculty Publications and Other Works -- Biochemistry, Cellular and Molecular Biology*.
https://trace.tennessee.edu/utk_biocpubs/92

This Article is brought to you for free and open access by the Biochemistry, Cellular and Molecular Biology at TRACE: Tennessee Research and Creative Exchange. It has been accepted for inclusion in Faculty Publications and Other Works -- Biochemistry, Cellular and Molecular Biology by an authorized administrator of TRACE: Tennessee Research and Creative Exchange. For more information, please contact trace@utk.edu.

Characterizing TMX and chemotactic receptor
arrays through bacterial two-hybrid and β -
galactosidase assays

Adam Hubler

University of Tennessee, Knoxville

College of Arts and Sciences

Department: Biochemistry & Cellular & Molecular Biology

Thesis advisor: Dr. Gladys Alexandre

Spring 2017

Acknowledgements

This project would not be possible if not for the unrelenting support from my advisors in the lab. First, I would like to thank Dr. Gladys Alexandre for the opportunity to participate in such a wonderful research lab and for her support throughout my research. Second, I would like to thank Jessica Gullett for her direction and vision with regards to this project; without her this project would merely be theory. Lastly, I would like to thank the other graduate students Lindsey O'Neil and Tanmoy Mukherjee and their numerous undergraduate assistants for their support and guidance.

Chapter I. Introduction to basic chemotaxis machinery and β -galactosidase assaying

Chemotactic signal cascades

As a survival mechanism, motile bacteria possess the ability to sense chemical gradients in their environments and bias their movements accordingly. This biased movement allows

bacteria to flock to beneficial, potentially metabolizable stimuli (attractants) or flee from harmful substances (repellants). The mechanism by which this biased

movement, this chemotaxis, occurs centers around a phosphorelay signal cascade comprised of transmembrane

chemoreceptors (MCPs), a baseplate array composed of multiple adapter proteins (CheW) and histidine-aspartate kinases (CheA), and a response regulator (CheY)

directly interfacing with flagellar motor machinery (Wadhams et al. 2004). Ligand

binding to chemoreceptors induces a conformational change in the MCPs

triggering CheA autophosphorylation.

Phosphorylated CheA's phosphate group is

then transferred by its kinase activity to the response regulatory CheY. Phosphorylated CheY

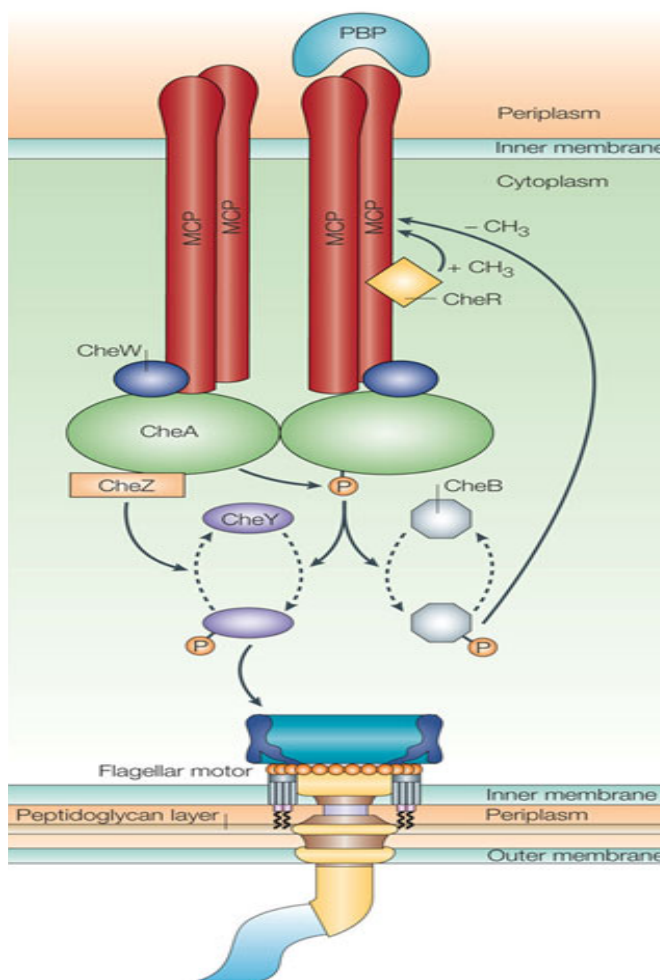


Figure 1. Basic chemotactic machinery including chemoreceptor MCPs, kinase molecule CheA, adapter protein CheW, response regulator CheY, as well as molecules not discussed CheR, CheZ, and CheB (Wadhams et al. Figure 2)

binds to the flagellar motor protein FliM, and subsequent reactions result in the switching of flagellar rotation causing the cell to “tumble.” When the cell senses through this tactic response that it is swimming toward beneficial chemicals, flagellar reversal occurs less frequently resulting in longer, straighter swimming paths. Conversely, if the motile cell swims past the positive source, the flagellar reversal frequency increases resulting in more frequent “tumbling” and reorientation. This research project centers around characterization of two distinct aspects of the chemotactic machinery in the model bacterium *Azospirillum brasilense*. *A. brasilense* chemotaxis signal transduction machinery is significantly more complex than that of *E.coli* and is representative of the complexity seen in the predicted chemotaxis systems in soil bacteria.

BACTH assay

Testing protein-protein interaction aids in elucidating functionality of novel domains or modeling organization of known domains (both explored in this project). Both qualitative and quantitative protein-protein interaction assays were used. To qualify protein interactions concerning chemotactic machinery, a bacterial adenylate cyclase two-hybrid (BACTH) system developed by Euromedex was used. Specialized for membrane-bound domains, the BACTH assay utilizes the interaction-dependent two-component reconstitution of the adenylate cyclase (CyaA) isozyme from *Bordetella pertussis*. The enzyme is inactive when the two fragments T25 and T18 are separated, but reconstitution restores activity and produces cyclic-AMP. The resulting cAMP binds to the catabolite activator protein (CAP), which in turn binds the promoter site on the *lac* operon, inducing transcription. By fusing two proteins X and Y to the complementary fragments, these proteins' interaction may be characterized based upon the activity of the *lac* operon.

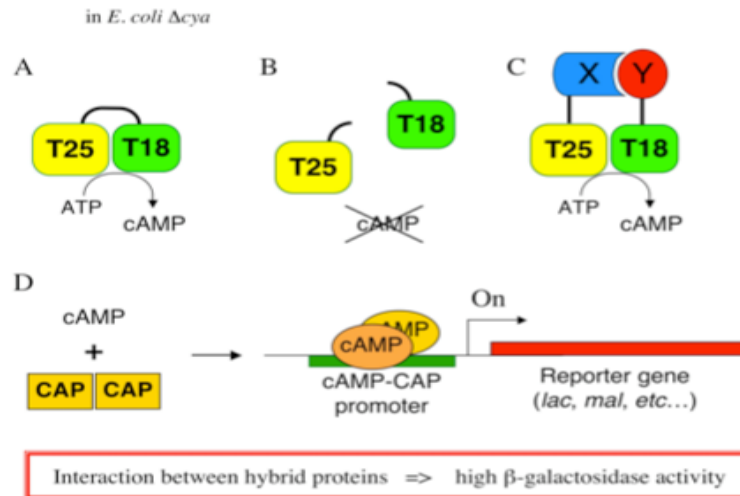


Figure 2. Reconstitution of CyaA's chimeric T25 and T18 fragments results in the CAP-mediated promotion of the *lac* operon

The two vectors used in testing protein-protein interactions were kanamycin-resistant, low-copy pKNT25 and carbenicillin-resistant, high-copy pUT18 with both plasmids' multiple cloning sites directly upstream from the cyclase fragments. By cloning the desired genes into the vectors, coexpression of the plasmids following cotransformation into competent cells allows for the testing of interaction. Ligated vectors pKNT25X or pUT18Y were transformed into XL1-blue competent cells, and subsequently the two isolated vectors were cotransformed into BTH101 competent cells. The interaction between proteins X and Y may be qualified through screening for lactose utilization on lactose enriched MacConkey agar. Colonies able to utilize lactose (i.e. colonies in which CyaA reconstitutes) develop a pink color compared to opaque colonies in the null population. MacConkey agar contains the pH indicator phenol red, which under acidic conditions turns a pink color. Catabolism of lactose depends on a functional CyaA, and thus only CyaA reconstitution produces a functional

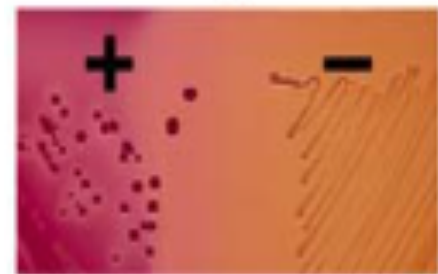


Figure 3. Positively interacting colonies grown on lactose enriched MacConkey agar show pink (left) compared to opaque, null colonies.

enzyme that allows lactose metabolism and the acidification of surrounding media, prompting the development of the pink color.

β-galactosidase assay

Following qualitative evaluation of protein-protein interactions through visual inspection of BACTH colonies, the same *lac* operon may be utilized to quantify the strength of protein-protein interaction. As the BACTH centered around lactose metabolism, β-galactosidase assays quantify protein-protein interaction through measurement of *lacZ* expression using β-galactosidase activity as a reporter. By inoculating cultures of colonies from the BACTH assay into liquid media and introducing a fluorescent substrate, the strength of interaction between the two sample proteins is derived by measuring the β-galactosidase activity. For this β-galactosidase assay, 4-methylumbelliferyl β-D-galactopyranoside (MUG) was used. This substrate, when cleaved by β-galactosidase, yields galactose and 4-methylumbelliferone, a fluorophore that absorbs light at approximately 360 nm and emits at 440 nm. The fluorescence of the sample, therefore, is directly correlated to β-galactosidase activity (i.e. *lac* operon output) and thus, protein-protein interaction strength (Ramsay 2013).

Chapter II. Characterizing novel domain TMX

Introduction

Chemotaxis is present throughout motile bacteria. *Azospirillum brasilense* is a rhizospheric bacterium that utilizes chemotaxis to move toward and ultimately colonize roots of cereals, providing a commensal benefit to the plant. *A. brasilense* possesses four distinct chemotactic operons (Che1, 2, 3, and 4), each encoding putative chemotaxis systems with distinct signaling outputs, two of which are not related to chemotaxis. Two chemotaxis operons were previously shown to be essential for chemotaxis: Che1 affects transient changes in cell

swimming speed (Bible et al. 2012), while Che4 modulates transient changes in the flagellar reversal frequency (Mukherjee et al. 2016). Examination of the Che1 pathway led to the discovery of a novel, seven-pass transmembrane protein domain (hence referred to as TMX) fused to the chemotaxis histidine-aspartate kinase, named CheA1. Since prototypical chemotaxis histidine kinases are soluble proteins, the fusion of CheA1 to TMX would restrict the protein to the membrane. Recent work (Gullett et al. 2017) showed that the fusion of TMX to the histidine kinase is a recent evolutionary event with TMX having no observable function in chemotaxis. In that study, CheA1 was also shown to be produced in two isoforms, a soluble isoform that functions as a prototypical chemotaxis signal transduction protein and a membrane-anchored isoform, the function of which is not known. In this project, the goal is to elucidate the protein-protein interactions network this protein (CheA1) and TMX are involved in. Intriguingly, TMX is a conserved protein in bacteria with most species having a single copy of this gene.

Previous work (Gullett, unpublished) showed that TMX mutant strains had membranes that were more rigid than the membrane of the wild type, with the mutant cells unable to adjust fluidity with changes in temperatures, implicating TMX in homeoviscous adaptation. When temperature increases or decreases, fluidity of the membrane must adapt to remain functional.

This is achieved through several mechanisms that lead to changes in the composition of the membrane. An optimal fluidity lies between staunch rigidity and porous permeability, and corresponds to the process of homeoviscous adaptation that refers to the mechanism by which cells maintain membrane fluidity

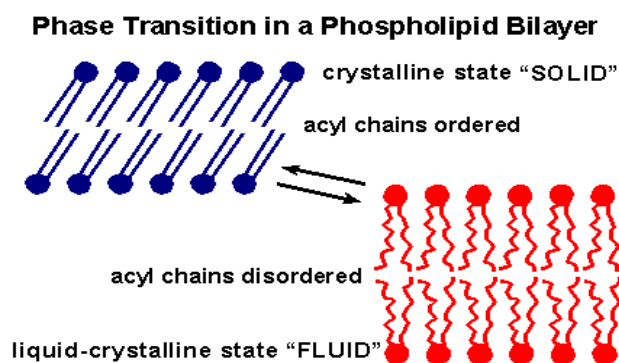


Figure 4. Altering acyl chain length and saturation affects membrane fluidity in response to external stimuli (Biological membranes 1998).

optimal with changing environmental conditions. When temperature increases, the membrane tends to become increasingly fluid causing the composition of the membrane to change in order to increase rigidity to compensate for this effect. Conversely, when the temperature falls, cells must shift toward more fluid membranes to maintain membrane function. Cells can control the fluidity of the membrane by changing both the chain length and saturation of fatty acid tails as well as changing the polar head group of the phospholipid (only the former two will be examined). Increasing the chain length or saturation of fatty acid tails cause the phospholipids to pack together, resulting in a more rigid membrane. Conversely, shorter, unsaturated fatty acid tails decrease Van der Waals forces between acyl chains, creating a more fluid membrane.

Further evidence supporting TMX's involvement in homeoviscous adaptation is its presence in the same regulon as the fatty acid biosynthetic (Fab) genes. Eight Fab genes are present in model *E. coli* (the model used in this project): FabA, B, D, F, G, H, I, and Z (Ernst et al. 2016). Each Fab gene controls various steps during fatty acid biosynthesis, including chain initiation, elongation, desaturation, and shuttling the fatty acid chain for introduction into the membrane. Furthermore, analysis of the phospholipids and fatty acid composition of a wild type strain of *Escherichia coli* and its derivative in which TMX encoding gene was deleted determined that fatty acid chain lengths and not phospholipids were affected by the mutation, suggesting a role for TMX in fatty acid biosynthesis. By affecting fatty acid biosynthesis, TMX could influence the composition of the membrane, and thus altering its fluidity. To further characterize the role of TMX in fatty acids biosynthesis, TMX interactions with the eight Fab proteins were tested using the BACTH and β -galactosidase assays.

Materials and Methods

In characterizing TMX, the BACTH assay was used to qualify its interactions with the Fab proteins. The positive control consisted of the interaction between pKNT25-*zip* and pUT18-*zip*. For both vectors, a leucine zipper is fused in frame with the CyaA fragment, and the leucine zipper dimerization results in reconstitution and a functional CyaA. The negative control consisted of the two empty vectors pKNT25 and pUT18.

Transformation into competent XL1-Blue cells. After cloning the respective genes into the vectors pKNT25 and pUT18, the plasmids were transformed into chemically competent XL1-Blue cells by first adding the entirety of ligation product into 50 μ L competent XL1-blue cells on ice and chilling the plasmid/cell mixture for thirty minutes. The contents were heat shocked at 42°C for forty-five seconds, and then replaced on ice for two minutes. 1 mL fresh LB liquid was added to each mixture, and the cells were shaken for one hour at 37°C. After growing, the cells were centrifuged at 8000 RPMs for three minutes, and 850 μ L of the supernatant was discarded. The remaining cells were resuspended and plated on LB solid agar plates. XL1-blue cells transformed with pKNT25X were plated on LB plates treated with kanamycin (50 μ g/mL), and those transformed with pUT18Y were plated on LB plates treated with carbenicillin (50 μ g/mL). Following transformation, the plasmids were isolated using a [©]Qiagen QIAprep spin miniprep kit protocol.

Cotransformation into competent BTH101 cells. 1 μ L of both pKNT25X and pUT18Y was introduced into 50 μ L chemically competent BTH101 cells and chilled on ice for twenty minutes. The plasmid/cell mixture was then placed in a 42°C heat bath for one minute and thirty seconds and replaced on ice for an additional minute. 1 mL warm, fresh LB broth was added to the tubes, and the cells were shaken at 37°C for one hour. The cells were centrifuged at 8000 RPMs for three minutes, and 850 μ L of the supernatant was discarded leaving approximately 150 μ L.

The remaining volume of newly cotransformed cells was spread across three LB plates supplemented with kanamycin (50 $\mu\text{g}/\text{mL}$) and carbenicillin (50 $\mu\text{g}/\text{mL}$) and incubated overnight at 37°C.

Adenylate cyclase activity assay. 5-7 of the isolated colonies for the experimental groups and controls were inoculated into 5 mL fresh LB with kanamycin (50 $\mu\text{g}/\text{mL}$) and carbenicillin (50 $\mu\text{g}/\text{mL}$). Three biological replicates of each interaction were conducted. The cultures were shaken overnight at 30°C, after which 2 μL samples were “spotted” onto MacConkey agar medium plates supplemented with lactose (10 g/L), kanamycin (50 $\mu\text{g}/\text{mL}$), and carbenicillin (50 $\mu\text{g}/\text{mL}$) poured into square, grid plates. Two rows of spotted samples were prepared for each biological replicate of the control interactions, while three rows for the three biological replicates of the experimental test interaction groups were included. Each row contained four technical replicates (an example is shown in **Figure 5A**).

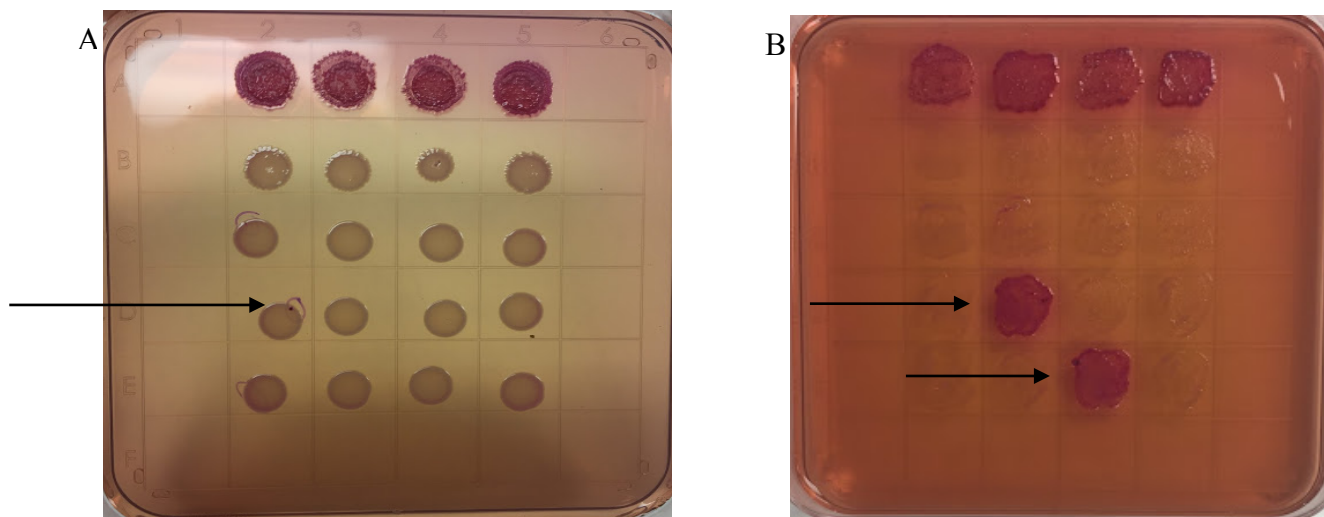


Figure 5. (A) The organization of “spotted” MacConkey plates was so that each row consisted of distinct biological replicates and each sequential column was an additional technical replicate. The arrow indicates what is to be expected for a positive interaction. (B) Each colony from the “spotted” MacConkey plate was “colored in” with an inoculating loop on the corresponding grid. The arrows indicate positive interactions. (Note: the images represent two different interactions)

The “spotted” plates were incubated at 30°C for 2-3 days until adequately grown. Potentially positive interactions were further isolated by taking an inoculating loop, dragging the tip of the loop through individual colonies (being sure to acquire positive spots), and re-streaking MacConkey agar plates supplemented with antibiotics as above followed by overnight incubation at 30°C. These interactions were visualized to estimate potential strength of interaction between TMX and the Fab proteins tested.

β-galactosidase assay. All three biological replicates of the controls and at least one technical replicate from the three experimental biological replicates of the re-streaked interaction mixtures grown on MacConkey plates were inoculated into 5 mL LB liquid cultures supplemented with the appropriate antibiotics. The liquid cultures were shaken overnight at 30°C until overgrown. The following day, 183 μL of each sample was reinoculated into 5 mL fresh LB liquid with antibiotics and shaken at 30°C until an optical density (OD₆₀₀) between 0.5 and 0.6 was reached. After reaching the appropriate OD₆₀₀, 100 μL from each sample and control was aliquoted into the wells of a 96-well microplate. Additionally, 100 μL plain LB liquid was aliquoted into separate wells to act as blanks. This 96-well plate was deemed the master plate. The OD₆₀₀ for the master plate was recorded using a microplate reader and saved for later analysis, and the master plate was placed in a -80°C freezer overnight.

To lyse the cells and access the cytoplasmic contents, the freeze-thaw method was used. Following overnight freezing, the master plate was placed directly into a 37°C incubator for thirty minutes with parafilm over the lid to prevent cross-contamination. Following the initial thawing, 10 μL from each well was aliquoted into a new 96-well plate using a multi-channel pipet. This new plate was deemed the assay plate and was replaced in -80°C for twenty minutes. The assay plate was once more thawed for fifteen minutes at 37°C. While performing the freeze-

thaw, the working reagent (1X MUG) was prepared by first making a 200X solution by dissolving 0.125 g 4-methylumbelliferyl β -D-galactopyranoside (MUG) into 2.5 mL DMSO and then diluting to 1X with 1X PBS. With cells lysed and reagent prepared, using a multi-channel pipet 100 μ L 1X MUG was added into each well, and the fluorescence at 440 nm was measured every two minutes for one hour using a plate reader.

Results

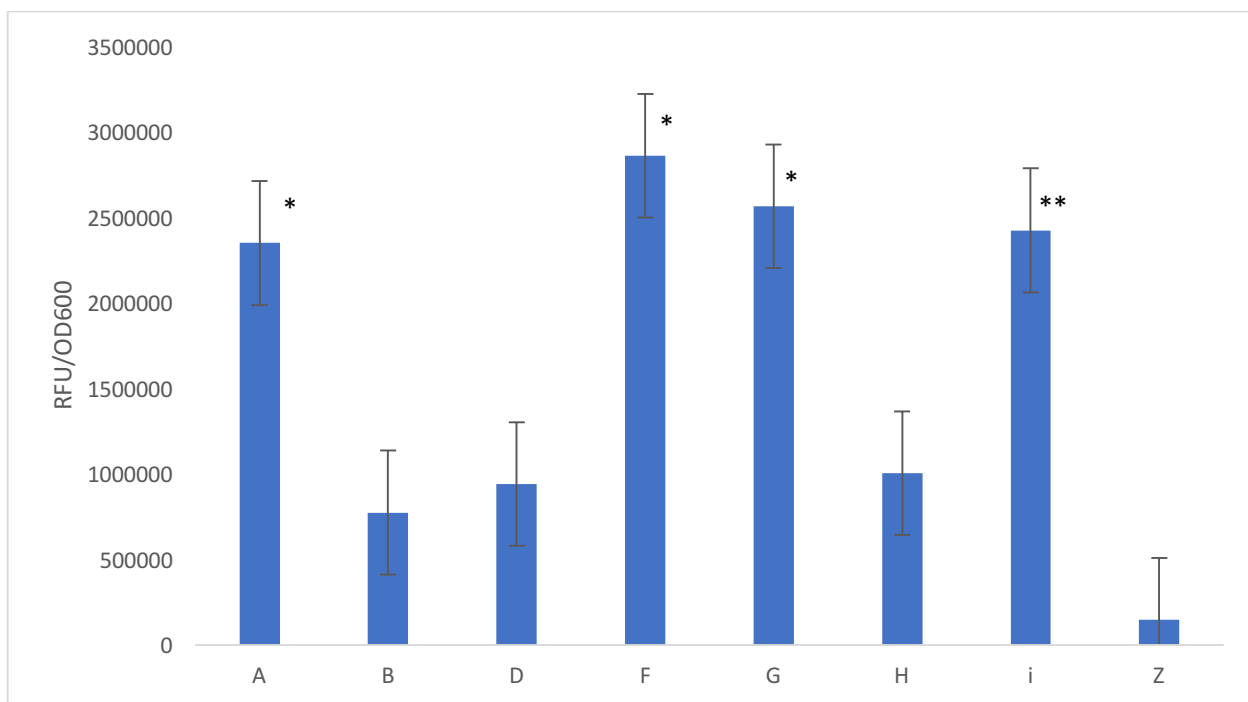


Figure 6. β -galactosidase activity in relative fluorescent units (RFUs) normalized with the OD₆₀₀ for each Fab protein's interaction with TMX in the low copy pKTN25. *= $p < 0.05$ **= $p < 0.0005$. Statistical significance was determined relative to the negative control analyzed on the same Petri plate.

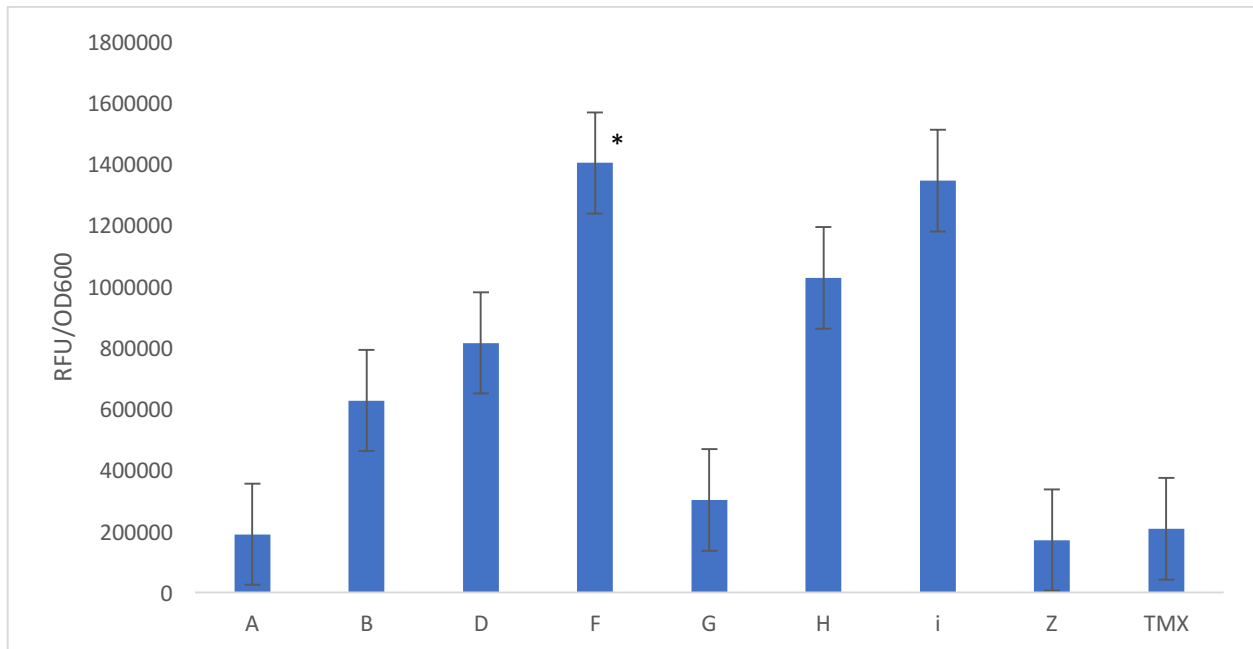


Figure 7. TMX's interaction in the high copy pUT18 with the Fab proteins in relative fluorescent units normalized with the OD_{600} . *= $p < 0.05$. Statistical significance relative to negative controls was determined using a T-test from the same assay plate.

Given that the gene coding for TMX is part of the FabR regulon and that the fatty acid chain lengths change in a mutant lacking TMX relative to wild type, we hypothesize that TMX regulates fatty acid biosynthesis by interaction with Fab enzymes. Data from β -galactosidase assays are shown in **Figure 6** and **Figure 7**. TMX interactions in the low copy pKNT25 yielded statistically significant interactions with FabA, FabF, and FabG with the most significant interaction being with FabI ($p < 0.0005$). In contrast, when expressed on the high copy pUT18 plasmid, only the TMX and FabF interaction was significant. Notably, TMX did not seem to interact with itself, and thus would function as a monomer (**Figure 7**).

Discussion

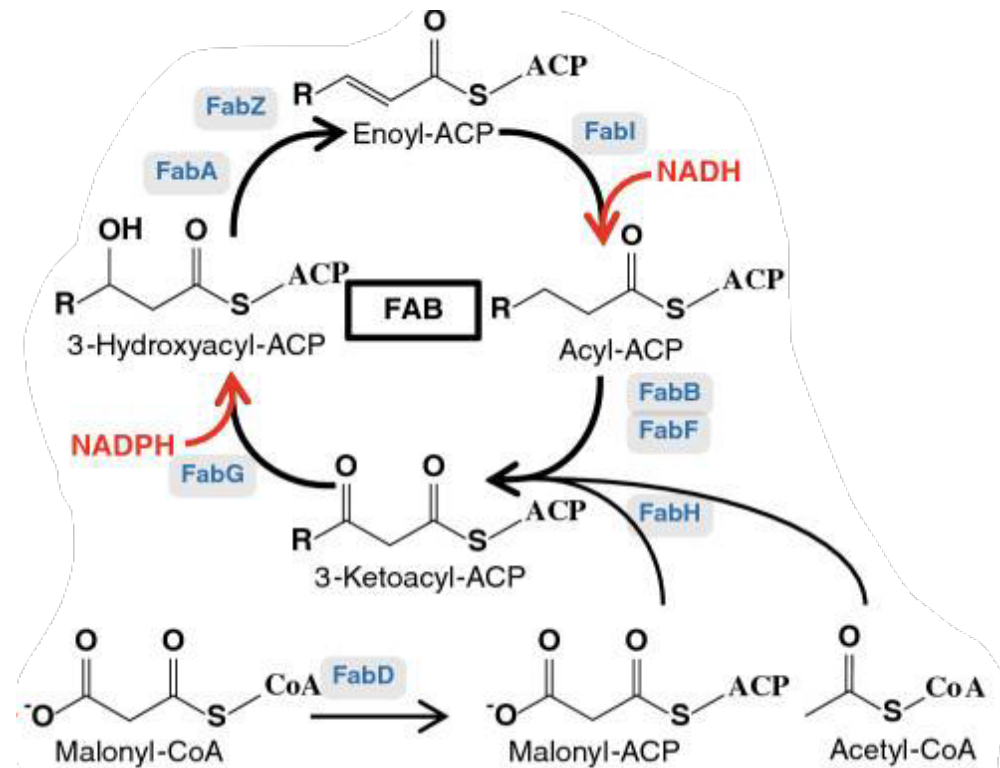


Figure 8. Fab genes control each step of fatty acid synthesis from initiation to elongation and shunting to the membrane for incorporation (Janßen et al. 2014 figure 3).

TMX targets long-chain fatty acid elongation. From malonyl-CoA to palmitic or stearic acid, fatty acids grow by addition of the two-carbon acetyl group for each completion of the elongation cycle (**Figure 8**). Initiation of fatty acid biosynthesis depends on FabD (Malonyl CoA:ACP transacylase), which activates Malonyl-CoA with the acyl carrier protein (Sreshty et al. 2012), followed by incorporation of this intermediate into the elongation cycle by FabH (Janßen et al. 2014). The fatty acid is then elongated two carbons at a time for fatty acid chains of certain lengths. While both FabF and FabB catalyze further elongation of the fatty acid chain, the two enzymes differ in their preference of fatty acid chain length. In *E. coli*, FabF is also unique in that it serves as a checkpoint for fatty acid biosynthesis, either shunting them for membrane incorporation or reinitiating another round of elongation. Our results show that TMX interacts strongly with FabF regardless of the copy number of the plasmid on which it is

expressed and insignificantly with FabB pointing to the domain's hand in intermediate to long-chain fatty acid synthesis.

TMX controls long-chain fatty acid profile additionally through FabG, FabA, and FabI sequestration. TMX manipulation of FabF alone could produce profound effects on membrane composition, but we found that TMX also interacted with the remaining fatty acid elongation enzymes. FabG (3-ketoacyl-ACP reductase) carries out the NADPH-dependent reduction of the newly condensed ketoacyl group. Subsequently, to control the fatty acid profile of a cell, FabG would be a necessary component. By influencing an enzyme yielding profiles rich in long-chain fatty acids, TMX may influence homeoviscous adaptation.

While fatty acid biosynthesis in *E. coli* utilizes a single 3-ketoacyl dehydrogenase, two different 3-hydroxyacyl dehydrases, FabA and FabZ, are present. The difference between the two enzymes lies in their substrate specificity. FabA primarily acts on unsaturated fatty acids; further study showed FabA is the primary dehydrase for intermediate to long-chain, saturated fatty acids (Janßen et al. 2014). FabZ shows preference for short-chain acyl groups. From our findings that TMX shows statistically significant interaction with FabA, but not with FabZ, our hypothesis that TMX impacts synthesis of long-chain fatty acids is supported given that FabA prefers long-chain fatty acids and FabZ prefers short-chain fatty acids.

TMX controls membrane contents through long-chain elongation inhibition. The quantitative evaluation of TMX's interactions with Fab enzymes using the β -galactosidase assay points to a mechanism by which TMX impacts the fatty acid profile of the cell. We propose that TMX influences a cell's membrane fatty acid profile by restricting the elongation of C-16 fatty acids to C-18 fatty acids through the activity of FabA, FabG, FabI, and FabF. Previous experimentation by Gullett et al. (unpublished) showed that the fatty acid profile for membranes

of *E.coli* ΔTMX strains contained more C-18 fatty acids compared to the wild type. Additionally, transferring these strains from 20°C to 37°C led to a change in the fatty acid membrane composition of the wild type strain, specifically in ratio of C-16 to C-18 fatty acids, but not that of the ΔTMX strain. This suggests that a lack of TMX leads to the production of longer chain fatty acids that are then incorporated into the membrane, increasing their rigidity. Furthermore, the wild type *E.coli* strain was shown to survive the temperature change while the mutant was not able to. Elevated concentrations of C-18 fatty acids point to TMX's role in affecting fatty acid chain length during synthesis. We propose that TMX's role in homeoviscous adaptation is one of enzymatic sequestration with respect to the biosynthetic enzymes FabA, FabG, FabI, and FabF. Sequestration of FabF, for example, would inhibit the synthesis of C-18 fatty acids by eliminating its catalytic capabilities, yielding the lower levels seen in the wild type when compared to the ΔTMX mutant strains (Gullett et al. unpublished).

Additionally, TMX's influence on multiple Fab enzymes allows for multiple points of control. Affecting output of any of the elongation enzymes (especially those involved in the long-chain elongation) would consequently affect the fatty acid profile of the cell membrane, controlling its fluidity.

These observations, while intriguing, remain to be confirmed using independent approaches, but together suggest a mechanism by which TMX could interact with certain Fab enzymes to alter fatty acid chain lengths.

Chapter III. Modeling chemotactic receptor arrays

Introduction

Chemotactic receptors form trimers of receptor dimers that localize to the cell pole via interaction with cytoplasmic proteins that form baseplate arrays (Aksenova 2014). Cryo-electron

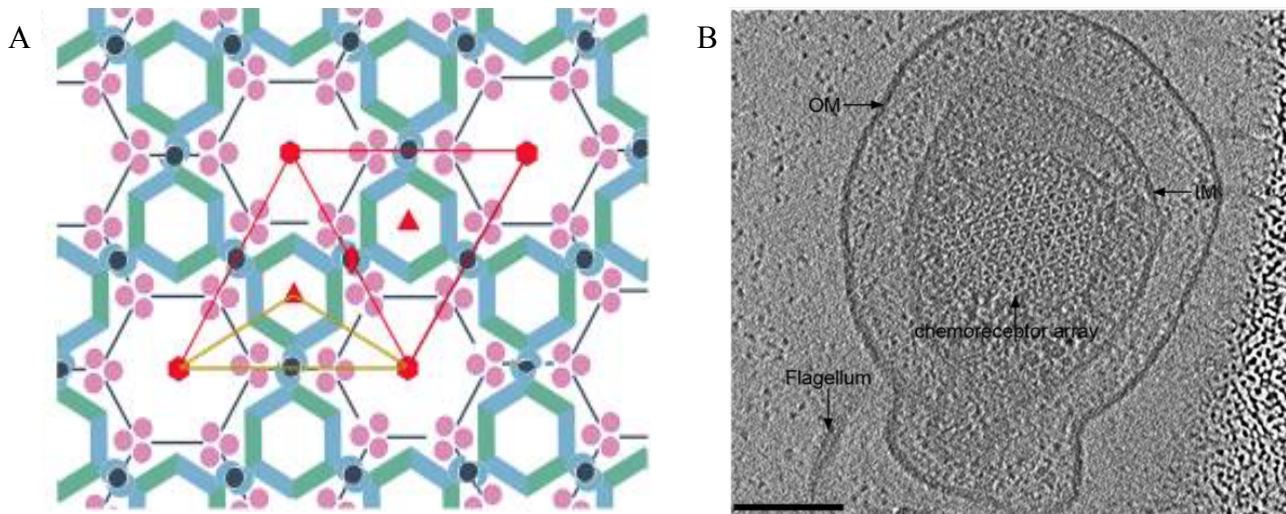


Figure 9. (A) depiction of chemotactic receptor arrays with CheW and CheA (blue and green) forming a lattice complexed with trimers of receptor dimers adjoined (pink). (B) Cryo-electron tomographic image of the chemotactic array lattice (Briegel et al. 2012).

tomography of *E. coli* chemotaxis arrays demonstrated that receptor arrays form lattices with a diameter of approximately 250 nm with hexagonal units consisting of the chemotactic histidine-aspartate kinase CheA and adapter protein CheW with the trimers of receptor dimers at the hexagonal vertices (Briegel et al. 2012) (**Figure 9**). While it is known that the chemotactic receptor array baseplates are composed of both CheA and CheW, the organization the two proteins exhibit in the baseplate is unknown. CheA exists in the cytosol as a dimer with both monomers linked by the P3 domain; its kinase activity is carried out by the P4 domain. CheW exists as a soluble monomer whose structure resembles the P5 domain of CheA (Wadhams et al. 2004). In examining the chemotactic baseplate arrays, Briegel et al. (2012) found that the hexagonal units appear to be arranged such that the CheW-like P5 binding domain of CheA and the CheW adapter protein alternate with the P4 kinase domain projecting toward the cytosol.

Chemotactic receptors (MCPs) are not structurally homogenous. MCPs differ with respect to the length of the C-terminal region of the receptor dimers, and chemotactic receptors may be grouped into classes depending on the length of the C-terminal regions. Sequence alignment across 152 genomes of

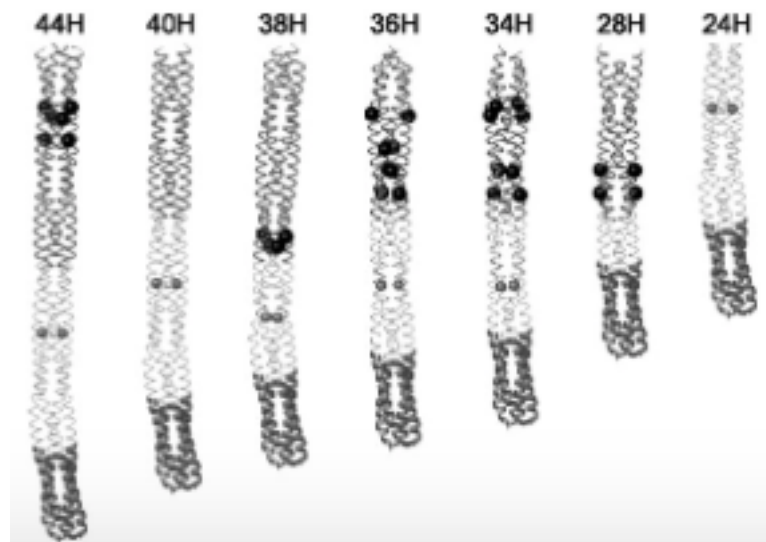


Figure 10. Representation of multiple sequence alignment depicting seven MCP classes. Cytosolic signaling domains are shown in dark, thick ribbons.

bacteria and archaea have grouped MCPs into 7 classes (Alexander et al. 2007). Two major MCPs present in *A. brasilense* are Tlp1, predicted to function largely in signaling to the Che1 pathway, and Tlp4a, encoded in the Che4 operon and thus predicted to signal via the CheA4 signaling pathway (Aksenova 2014). Previous experimentation has revealed that chemotaxis receptors form segregated clusters dependent on the length of their C-terminal region (Seitz et al. 2014). Tlp1 and Tlp4a represent two distinct classes of chemotactic receptors, and as such we can predict that they will form distinct clusters.

In characterizing the structure of chemotactic receptor arrays, it is important to determine the organization of CheA and CheW proteins in the baseplate arrays, as well as determining if crosstalk is exhibited by the CheA and CheW proteins from both Che1 and Che4 pathways. Additionally, it may be possible that the components of receptor arrays are recruited stochastically as opposed to a strict organization. Briegel et al. (2012) suggests that a baseplate unit may even be composed entirely from CheW proteins as opposed to the previously proposed

Quantification of protein-protein interactions are shown in **Supplementary figures 12-15.**

CheA/CheW baseplate interactions. In testing chemoreceptor baseplate proteins CheA and CheW from both Che1 and Che4 we found that both CheA1 and CheA4 significantly interact with themselves and with their homologs in all circumstances except for when CheA1 is in the high copy pUT18. Additionally, CheW4 interacted with itself very strongly, contrasting with CheW1 that did not. Further, CheW1 only interacted with CheW4 when CheW1 was in the high copy plasmid. Finally, when testing interactions between CheA1, CheA4, CheW1, and CheW4, all interactions were significant except for when CheA1 expression was low and in testing CheA4 in the high copy with CheW4 in the low copy.

Chemoreceptor interactions. Tlp1 and Tlp4a did not interact significantly with each other. Interestingly, in testing the self-interactions of Tlp1 and Tlp4a, only Tlp1 was found to dimerize, but not Tlp4a.

Baseplate interactions with chemoreceptors. Tlp1 was found to interact strongly with CheA1 and CheW1 but did not interact with CheA4 and CheW4, irrespective of plasmid copy number. Similarly, Tlp4a interacted with CheA4 and CheW4 as well as CheA1, but only when expressed from the high copy vector, suggesting dosage effects.

Discussion

Che1 and Che4 baseplate proteins exhibit crosstalk. β -galactosidase assays of protein-protein interactions revealed significantly positive interactions between baseplate proteins CheA1, CheA4, CheW1, and CheW4. As both CheA1 and CheA4 interactions with themselves were significant, so too was CheA1's interaction with CheA4, though only when CheA1 was

expressed from the high copy vector. This discrepancy may be due to the fact that CheA1 has two isoforms: a membrane bound form that does not function in chemotaxis, and a soluble CheA1 form that is much less abundant and functions as a prototypical CheA (Gullett et al, submitted). We hypothesize that the presence of the two isoforms confounds the interactions of CheA1 with other proteins because only when CheA1 is produced from a high copy vector would any interaction be detected that could

correspond to the prototypical soluble CheA1. With the baseplate proteins capable of interacting with components of each of the two operons, it is logical to conclude that chemoreceptor baseplate arrays may be composed of proteins solely from the same chemotactic pathway or from both pathways, supporting the hypothesis of crosstalk in the chemotactic signaling cascade (**Figure 11**).

CheW plays an additional structural role in receptor arrays. CheA1 and CheA4 interacted significantly with one another, while CheW1 did not interact with itself. Both findings were anticipated given CheA's dimeric nature and CheW's monomeric existence (Wadhams et

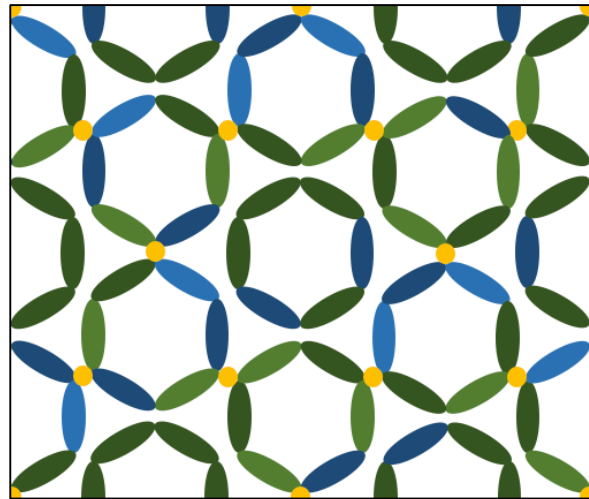


Figure 11. Chemotactic receptor array baseplates form hexagonal lattices composed of alternating CheA (light) and CheW (dark) proteins from either Che1 (blue) or Che4 (green) pathways linked by the CheA P3 domain (yellow). Additionally, CheW-only structural units lie in the center of the hexagonal lattice.

al. 2004). However, an extremely significant ($p < 0.0005$) interaction was found when testing CheW4's interaction with itself. These findings would be consistent with the hypothesis put forth by Briegel et al. (2012) that certain hexagonal baseplate units are solely comprised of the adapter protein CheW. Without a CheA present, such units would be incapable of signaling in the chemotactic pathway, but these rings could function as structural units, stabilizing the receptor arrays as conformational changes occur during signaling. Additionally, these units would be distinct from the functional baseplate machinery as it is unable to couple to adjacent units without a CheA P3 domain present. **Figure 11** depicts these CheW-only rings in the center of the functional hexagonal lattice, composed of CheW1 and CheW4. It is important to note that, given the findings of this project, CheW4 proteins may exist adjacent to one another, but CheW1 cannot.

Tlp1 and Tlp4a prefer specific chemotactic pathways. The two chemotactic receptors showed preferred interactions with Che1 or Che4 proteins. Tlp1 has been previously implicated in signaling to the Che1 pathway, and its significant interaction with Che1 baseplate proteins supports that hypothesis. Likewise, Tlp4a preferentially interacted with Che4 baseplate proteins—an expected finding given the gene coding for Tlp4a's location within the Che4 operon.

Comparing the two receptors' pathway biases with data supporting crosstalk between baseplate proteins yields a clearer concept of chemotactic receptor arrays. Though the lattice of hexagonal baseplate units may be comprised of either Che1 or Che4 proteins, the trimer bundles of receptor dimers dock at specific points of the polar arrays. Further, data reveals that Tlp1 and Tlp4a are segregated from one another. Given the differences in the receptors' sizes, it is logical to conclude that heterogeneous clusters could not form. However, though the different receptors

do not interact, the baseplate proteins exhibit crosstalk, and so receptor clusters may be composed of interspersed, though segregated, Tlp1 and Tlp4a bundles.

Interestingly, Tlp4a did not interact with itself, which is unusual given that literature states bacterial chemoreceptors form homodimers (Seitz et al. 2014). This discrepancy may be attributed to shortcomings in the experimental design. While Tlp4a showed preference for CheA4 and CheW4 (as well as CheA1) in the high-copy pUT18 vector, the receptor when expressed on the low-copy pKNT25 vector showed no statistically significant interactions at all, possibly pointing to issues with the N-terminal T25 fusion. To fully elucidate the nature of Tlp4a interactions with baseplate machinery in chemotactic receptor arrays, it would be beneficial to retest the interactions with the receptor fused to the T25 fragment's C-terminus. Additionally, Tlp1 was shown to only statistically interact with Che1 proteins. While this finding supports previous hypotheses concerning the receptor's signaling to the Che1 signaling pathway, its lack of statistically significant interactions with CheW4 would exclude the trimer of receptor dimers from interacting with the structural CheW unit. With the absence of evidence supporting Tlp4a's dimerization and Tlp1's lack of interaction with the CheW structural units, we lack the data needed for accurately modeling the two receptors' interactions with the baseplate machinery.

Chemotactic receptor arrays stochastically form mixed Che1/Che4 clusters with specified receptor docking. The findings obtained here support the hypothesis that chemotactic receptor arrays form lattice-shaped clusters at the poles with baseplate proteins CheA1, CheA4, CheW1, and CheW4 stochastically recruited for assembly and with the receptor's C-terminal signaling domain's length ensuring segregation of the clusters according to size (Seitz 2014). The hexagonal CheA/CheW units composed of either Che1 or Che4 proteins are joined at the vertices through the homodimerization of adjacent CheA P3 domains (Briegel et al. 2012).

Additionally, Tlp1 and Tlp4a dock to form segregated functional units with Che1 and Che4, respectively. It is important to note that Cryo-EM images of *A. brasilense* wild type, $\Delta che1$, and $\Delta che4$ mutants all assemble two intact clusters, while only the double $\Delta che1\Delta che4$ mutant lacks any visible chemotaxis clusters. This observation supports the hypothesis that any of the Che1 or Che4 baseplate proteins can nucleate polar cluster formation.

Supplementary Figures

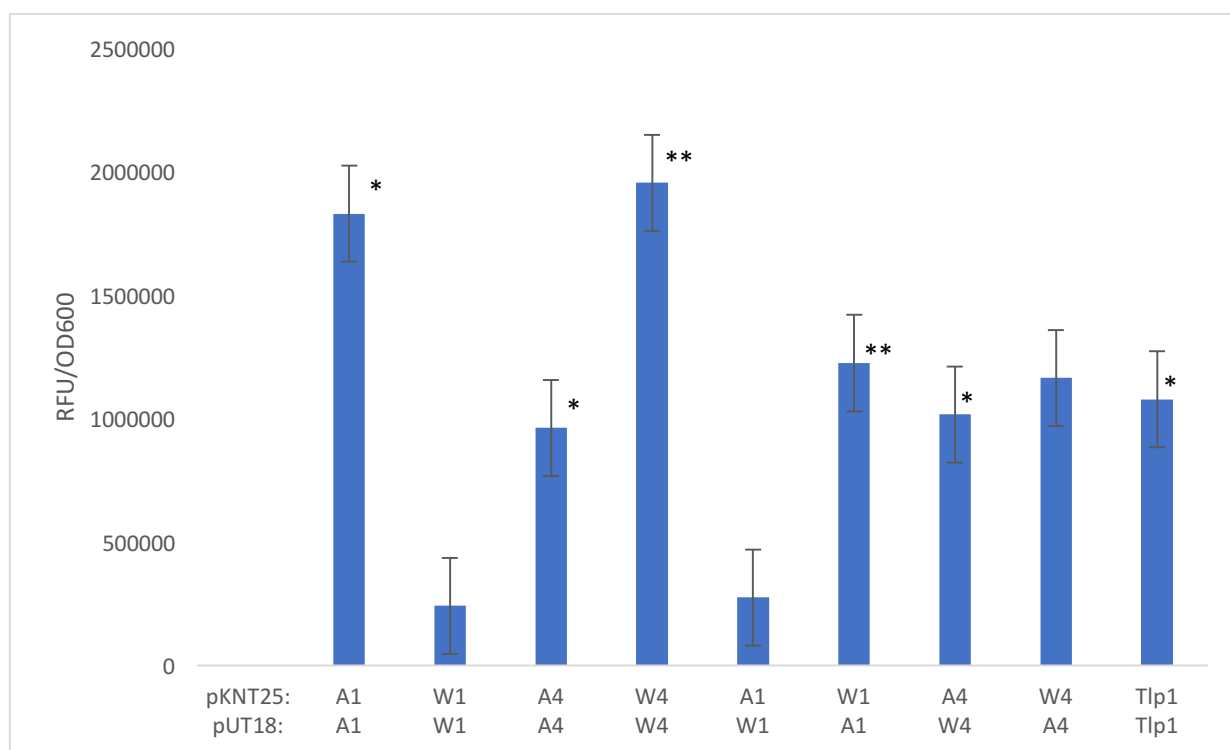


Figure 12. β -galactosidase data displaying relative fluorescent units (RFUs) normalized with optical density (OD_{600}). Protein-protein interactions are displayed with their respective vector pKNT25 and pUT18 on top and on bottom. * = $p < 0.05$ ** = $p < 0.0005$. Asterisks denote significance with respect to the negative control from the respective master plate.

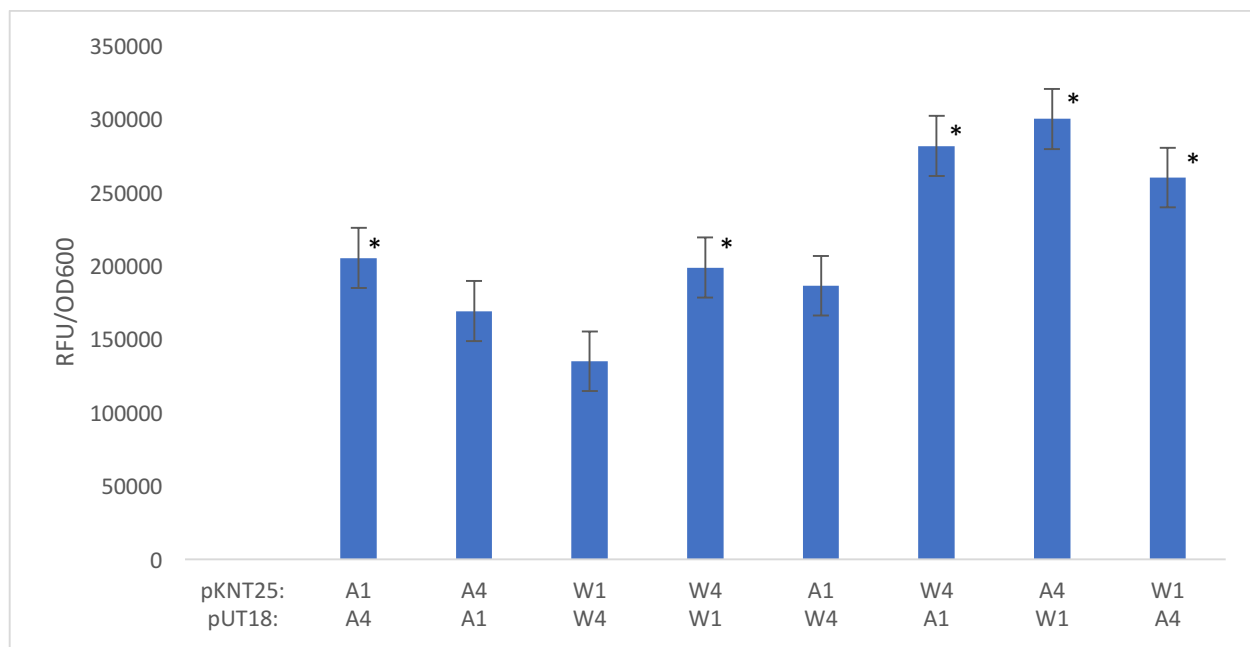


Figure 13. β -galactosidase data displaying relative fluorescent units (RFUs) normalized with optical density (OD_{600}). Protein-protein interactions are displayed with their respective vector pKNT25 and pUT18 on top and on bottom. * = $p < 0.05$ ** = $p < 0.0005$. Asterisks denote significance with respect to the negative control from the respective master plate.

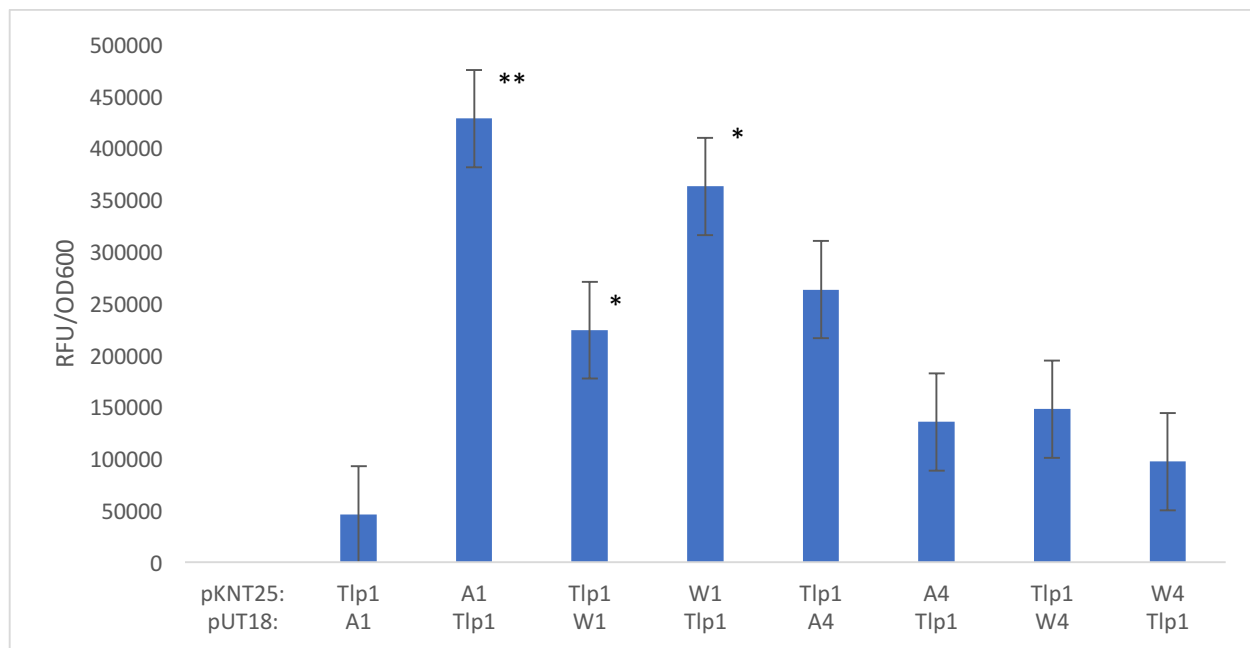


Figure 14. β -galactosidase data displaying relative fluorescent units (RFUs) normalized with optical density (OD_{600}). Protein-protein interactions are displayed with their respective vector pKNT25 and pUT18 on top and on bottom. * = $p < 0.05$ ** = $p < 0.0005$. Asterisks denote significance with respect to the negative control from the respective master plate.

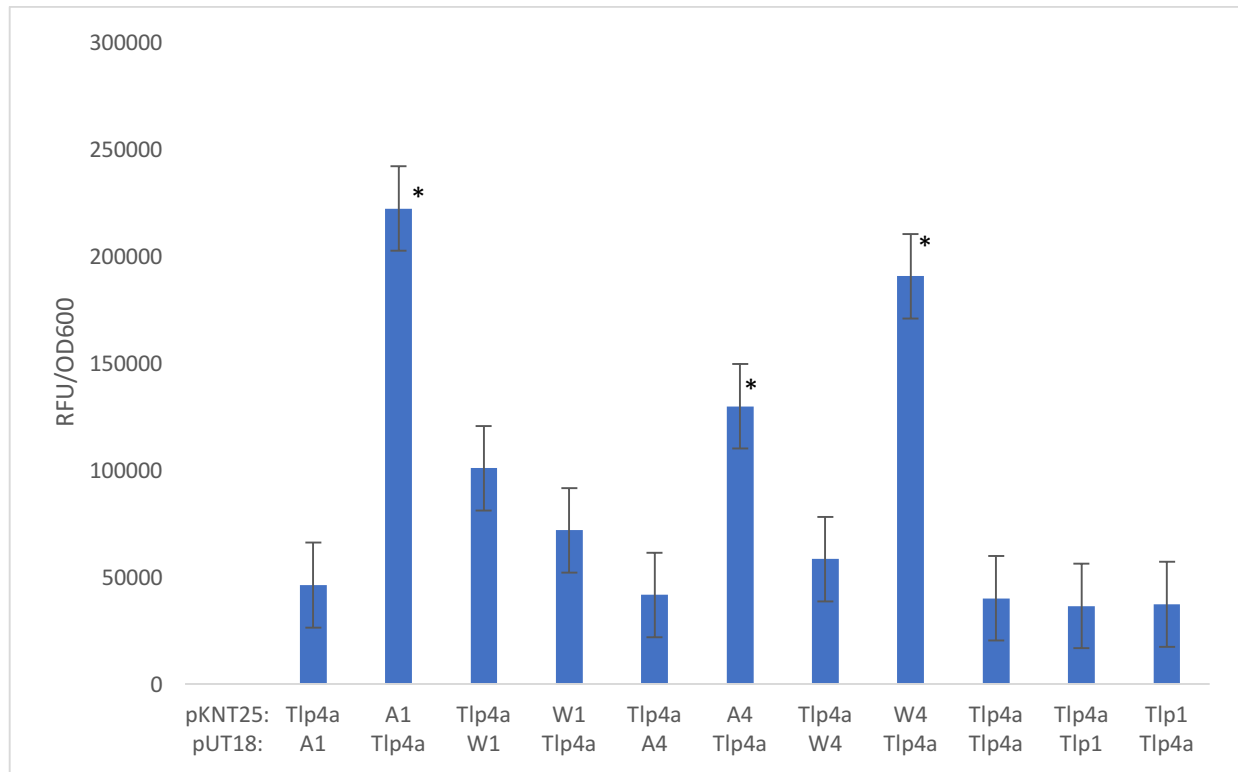


Figure 15. β -galactosidase data displaying relative fluorescent units (RFUs) normalized with optical density (OD_{600}). Protein-protein interactions are displayed with their respective vector pKNT25 and pUT18 on top and on bottom. * = $p < 0.05$ ** = $p < 0.0005$. Asterisks denote significance with respect to the negative control from the respective master plate.

References

- Aksenova, A. (2014). Localization of chemoreceptors in *Azospirillum brasilense* (published thesis). University of Tennessee, Knoxville.
- Alexander, R. P., & Zhulin, I. B. (2007). Evolutionary genomics reveals conserved structural determinants of signaling and adaptation in microbial chemoreceptors. *Proceedings of the National Academy of Sciences of the United States of America*, 104(8), 2885–90.
- Bible, A., Russell, M., & Alexandre, G. (2012). The *Azospirillum brasilense* Che1 Chemotaxis Pathway Controls Swimming Velocity, Which Affects Transient Cell-to-Cell Clumping. *Journal of Bacteriology*, 194(13), 3343-3355.

- Briegel, A., Li, X., Bilwes, A., Hughes, K., Jensen, G., & Crane, B. (2012). Bacterial chemoreceptor arrays are hexagonally packed trimers of receptor dimers networked by rings of kinase and coupling proteins. *Proceedings of the National Academy of Sciences*, 109(10), 3766-3771.
- Ernst, R., Ejsing, C., & Antony, B. (2016). Homeoviscous Adaptation and the Regulation of Membrane Lipids. *Journal of Molecular Biology*, 428(24), 4776-4791.
- Gullett, J., Bible, A., Alexandre, G. (2017). Distinct domains confer CheA with unique functions in chemotaxis and cell length in *Azospirillum brasilense* Sp7. *Journal of Bacteriology*, 199(9).
- Held, P. (2001). β -Galactosidase Activity Determination using a BioTek Microplate Fluorescence Reader. *BioTek*.
- Janßen, H. J., Steinbüchel, A. (2014). Fatty acid synthesis in *Escherichia coli* and its applications towards the production of fatty acid based biofuels. *Biotechnology for Biofuels*, 7(7), N.P.
- Jeon, E., Lee, S., Han, S. O., Yoon, Y. J., & Lee, J. (2012). Improved production of long-chain fatty acid in *Escherichia coli* by an engineering elongation cycle during fatty acid synthesis (FAS) through genetic manipulation. *Journal of Microbiology and Biotechnology*, 22(7), 990-999.
- Mukherjee, T., Kumar, D., Burriss, N., Xie, Z., & Alexandre, G. (2016). *Azospirillum brasilense* Chemotaxis Depends on Two Signaling Pathways Regulating Distinct Motility Parameters. *Journal of Bacteriology*, 198(12), 1764-1772.
- N.A. (1998). Biological Membranes. *Department of Physical and Macromolecular Chemistry, Charles University*.

- Ramsay, J. P. (2013). High-throughput β -galactosidase and β -glucuronidase Assays Using Fluorogenic Substrates. *Bio-protocol*, 3(14).
- Seitz, M. K. H., Frank, V., Massazza, D. A., Vaknin, A., and C. A. Studdert (2014). Bacterial chemoreceptors of different length classes signal independently. *Molecular Microbiology*, 93(4), 814-822.
- Sreshty, M. A. L., Surolia, A., Sastry, G. N., & Murty, U. S. (2012). Deorphanization of Malonyl CoA:ACP Transacylase Drug Target in Plasmodium falciparum (PfFabD) Using Bacterial Antagonists: A 'Piggyback' Approach for Antimalarial Drug Discovery. *Molecular Informatics*, 31(3), 281-299.
- Wadhams, G. H., & Armitage, J. P. (2004). Making sense of it all: bacterial chemotaxis. *Nature Reviews. Molecular Cell Biology*, 5(12), 1024-37.